Available online at www.sciencedirect.com
ScienceDirect
Earth and Planetary Science Letters 258 (2007) 414–427
EPSL
www.elsevier.com/locate/epsl

Chemical weathering, mass loss, and dust inputs across a climate by time matrix in the Hawaiian Islands

Stephen Porder [a,*,1], George E. Hilley [a], Oliver A. Chadwick [b]

[a] Department of Geological and Environmental Sciences, Stanford University, Stanford, CA 94305, USA
[b] Department of Geography, University of California, Santa Barbara, CA, 93106, USA

Received 15 November 2006; received in revised form 28 March 2007; accepted 28 March 2007
Available online 4 April 2007
Editor: M.L. Delaney

Abstract

We determined the total mass loss and rate of chemical weathering from three minimally eroded, Hawaiian lava flows that are ~10, 170, and 350 ka old. Using a backhoe, we sampled the entire weathering zone at 28 sites and measured the depletion or enrichment of each major element in each soil horizon relative to parent material. We were able to assess the influence of both climate and substrate age on chemical weathering because each flow crosses a precipitation gradient from ~600 to ~2500 mm yr^{-1}. Mass loss rates were highest for the 0–10 ka interval under the wettest climatic conditions (54 t km^{-2} yr^{-1}), and decreased to near zero in the wet sites during the 10–170 and 170–350 ka intervals. Not surprisingly, weathering rates were lower in drier sites; ~24 t km^{-2} yr^{-1} from 0–10 ka to <2 t km^{-2} yr^{-1} thereafter. However the effects of precipitation were non-linear. There was a precipitation threshold below which mass loss was relatively small, and above which mass loss was substantial but insensitive to increased rainfall. Chemical weathering rates depend on tectonic uplift, erosion, climate, rock type or some combination thereof. By working on stable, uneroded surfaces of a single rock type across a well-constrained precipitation gradient, we were able to identify another potential driver: the rate of dust deposition. Although Hawai'i is one of the least dusty places in the northern hemisphere, dust inputs reached 82% of the total mass loss from the weathering zone at some sites, and averaged 30% on the 170 ka flow. This highlights the potential importance of dust as a component of observed weathering fluxes from catchments worldwide.

Keywords: weathering rate; mass loss; Hawai'i; dust; chemical depletion; climate; age

1. Introduction

Chemical weathering of silicates is a major sink for atmospheric CO_2 over geologic timescales and modulates Earth's climate (Berner et al., 1983; Raymo and Ruddiman, 1992; Jacobson and Blum, 2003). Biogeochemical shifts associated with rock weathering and soil development have profound effects on ecosystem productivity (Chadwick et al., 1999; Vitousek, 2004; Wardle et al., 2004). However, quantifying the rate of chemical depletion for a given substrate over geologic time is a complicated endeavor, in part because chemical weathering is often strongly coupled with physical erosion (Riebe et al., 2004; Von Blanckenburg, 2005),

* Corresponding author. Tel.: +1 401 863 6356; fax: +1 401 863 2166.
E-mail address: stephen_porder@brown.edu (S. Porder).
[1] Current address: Department of Ecology and Evolutionary Biology, Brown University, Providence, RI 02912, USA.

0012-821X/$ - see front matter © 2007 Elsevier B.V. All rights reserved.
doi:10.1016/j.epsl.2007.03.047

and in part because it is difficult to quantify losses from the entire weathering profile between the surface and unweathered parent material at depth (but see Anderson et al., 2002).

Three techniques have commonly been applied to measure rates of chemical weathering: quantification of mass loss from minimally eroded soils of known age (i.e. chronosequences; e.g. Jenny, 1941; Taylor and Blum, 1995), catchment-scale river sampling (e.g. White and Blum, 1995; Riebe et al., 2004; Likens, 2004), and laboratory experiments (e.g. White and Brantley, 2003). All three approaches are subject to considerable uncertainly. Measurement of mass loss from chronosequences depends on accurate characterization of well dated, unweathered parent material, finding surfaces for which physical erosion has been minimal, quantifying atmospheric inputs of dust, and relying on an assumption of immobility of certain elements (usually a trace metal) to account for soil dilation or contraction. Stream sampling is a more common approach, but assumes groundwater flux out of a catchment is minimal (but see Basu et al., 2001), requires accurate discharge data and element concentration data from a variety of flow regimes over time (Stallard, 1995; White and Brantley, 1995), and must accept the uncertainties of extrapolating short-term measurements to long-term rates. This is particularly problematic given substantial recent human alteration of most of the Earth's surface as well as the accumulation of nutrients in post-disturbance vegetation (Von Blanckenburg, 2005; Wilkinson, 2005). Laboratory measurements are by necessity short term, and often produce results that are at odds with field measurements. Nevertheless recent work has made strides in understanding these differences, and suggests that in the absence of physical removal of weathered material, weathering rates decline exponentially with time (White and Brantley, 2003).

Quantifying chemical weathering rates is a first step, but to understand potential feedbacks to climate and biogeochemical cycles it is necessary to determine the factors that control these rates. Several studies have used catchment-scale river fluxes to infer the global drivers of chemical weathering, and have argued that rates of chemical weathering are related to a combination of uplift and erosion (Jacobson and Blum, 2003; Jacobson et al., 2003; Riebe et al., 2004; Carey et al., 2005), parent material composition (Bluth and Kump, 1994; Gíslason et al., 1996) and climate (White and Blum, 1995; Jacobson et al., 2003; Riebe et al., 2004). Nevertheless, the drivers of chemical weathering remain a subject of vigorous debate, summarized recently by Von Blanckenburg (2005). We note that the weathering literature has not emphasized atmospheric import of exogenous material (i.e. dust and/or marine aerosols) as a potential source of highly weatherable material to watersheds and thus a control on rates of chemical weathering. However on older land surfaces atmospheric inputs can be of a similar magnitude as watershed outputs (for example, roughly one-third for old, dust-poor but marine-aerosol rich Hawaiian landscapes; Kurtz et al., 2001; Hedin et al., 2003).

We quantified mass loss by comparing minimally eroded soils to unweathered parent material on three basaltic lava flows on the Island of Hawai'i. Three facets of our approach combine to produce a unique dataset that is particularly well-suited to understanding the effects of surface age and climate on rates of chemical depletion within the weathering zone. First, these flows are well dated (10, 170, and 350 ka) and cross a precipitation gradient that ranges from ~600 to 2500 mm yr^{-1} in <10 km on the leeward side of the island. Thus they can be thought of as a chronosequence of climosequences. Second, we sampled the entire weathering zone (from the soil surface to unweathered bedrock) from a total of 28 sites, arrayed across the age and rainfall gradients. Third, we were able to identify and quantify exogenous dust in the weathering zone. We took advantage of the orthogonal variation in parent material age and climate to ask the following questions: 1) What are the rates of mass loss from basaltic lavas under a suite of different climatic conditions? 2) How do these rates compare with those calculated from catchment-scale measurements? and 3) How does the mass of added dust (blown predominantly from the deserts of Asia) compare to the mass lost via chemical weathering?

2. Site description

We sampled three basalt lava flows — aged ~10, 170, and 350 ka that descend in elevation from about 1200 m to <50 m on the leeward side of Kohala mountain on the island of Hawai'i (Fig. 1). The youngest flow is on the Mauna Loa volcano, near Kainaliu on Hawai'i's Kona Coast; the older flows are on Kohala Mountain, which forms a peninsula on the northern tip of the island. Annual rainfall is strongly affected by orographic effects, rainfall decreases from ~2500 mm yr^{-1} in the upper elevations to as little as 200 mm yr^{-1} downslope (Giambelluca et al., 1986). In the past, the rainfall gradient may have been less extreme due to lower rainfall at the wetter end of the gradient, but for the entire history of these flows there has been an orographic gradient similar in direction, if not magnitude, to what exists today (Hotchkiss, 1998; Hotchkiss et al., 2000;

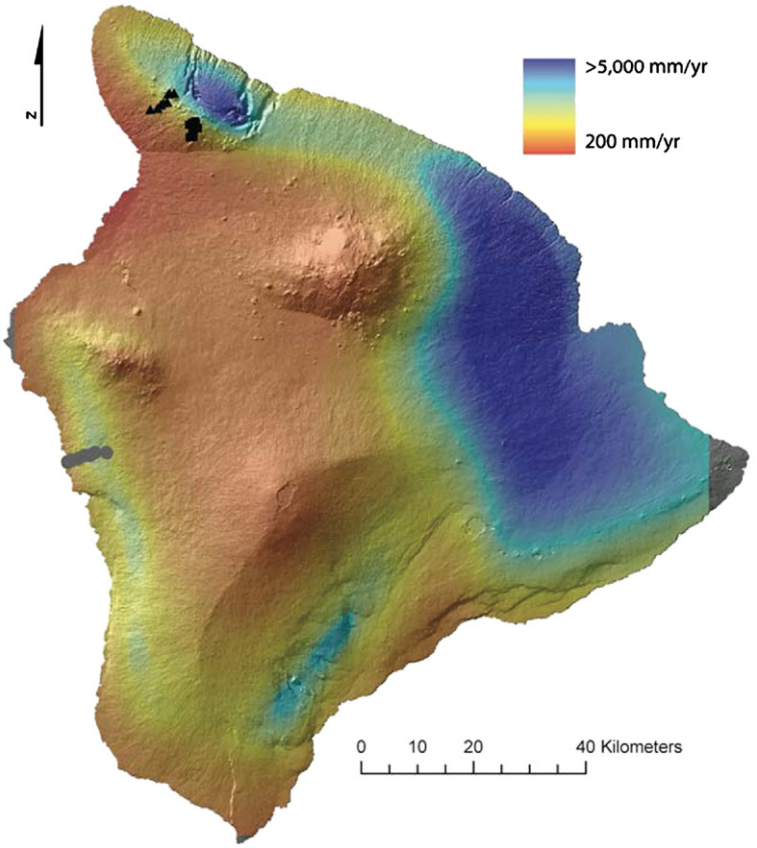

Fig. 1. Location of the three sampled lava flows overlaid on a shaded relief map of the Island of Hawai'i. The color scale shows the extreme, topographically driven rainfall gradients across the flows. Light grey symbols are the 10 ka (Kona) transect, dark grey are 170 ka (Hawi) and black are 350 ka (Pololu). Sampling locations are based on field GPS measurements, rainfall data from the state of Hawai'i rainfall map (contours interpolated in ArcGIS 9.0), elevation data from USGS DEM. Areas with no rainfall color are where interpolation of rainfall contours failed to return a result in ArcGIS.

Chadwick et al., 2003). Temperatures rise from 16 °C at the higher altitude, wetter sites to 24 °C at the low altitude, drier sites, based on an empirically derived lapse rate for Hawai'i (Giambelluca and Schroeder, 1998). Potassium–argon (K–Ar) dating and petrologic analysis reveal that the oldest flow is comprised of tholeiitic flows (Pololu Volcanics) ranging in age from 470 to 220 ka (McDougall, 1964; McDougall and Swanson, 1972; Spengler and Garcia, 1988; Chadwick et al., 2003). The intermediate aged flows are alkalic a'a flows (Hawi Volcanics) ranging from 230 to 110 ka. More details on dating methodology and errors are provided in Chadwick et al. (2003). The youngest flow is a'a, tholeiitic in composition, and dated at ~10 ka based on radiocarbon dating of charcoal extracted from beneath the flow (Wolfe and Morris, 1996). All of the flows exhibit the characteristic gentle (<15°) slope of a Hawaiian shield volcano, and there is no significant stream development near the sites. We sampled slightly concave locations in overall convex portions of the landscape in order to minimize the impact of local erosion and deposition processes (see Chadwick et al., 2003). In the absence of a transport mechanism other than soil creep and wind erosion, and considering the gentle slope, we believe that physical erosion of these surfaces has been minimal, especially after the initial colonization of the flows by vegetation. The sites were once dominated by Hawaiian lowland dry and mesic forest, but are now mostly dominated by exotic species (cacti, *Opuntia* spp., grasses like Kikuya, *Pennisetum clandestinum*, Buffel Grass *Cenchrus ciliaris*, the native lovegrass *Eragrostis variablilis* and the low tree Keawe *Prosopsis* spp) (McEldowney, 1983; Chadwick et al., in press).

Soil development on Hawaiian a'a basalt flows initially occurs primarily in fine-grained tephra and organic material that blows into crevices around the larger clinkers. As water gradually weathers the fines and

clinkers, surface soils develop and the weathering zone propagates downward into the flow (O.A. Chadwick, pers. obs.). Later in soil development exogenous dust, blown largely from Asian deserts, becomes a significant fraction of the surface horizons on uneroded flows (Kurtz et al., 2001). Downward propagation of the weathering front on pahoehoe flows is much slower, because of their lower permeability and weatherable surface area. This can be seen in the difference in weathering between interfingered, similarly aged, a'a and pahoehoe flows around the island of Hawai'i (S. Porder, pers. obs.). Our three flows are all a'a/tephra, although the weathering zone on the wetter part of the oldest flow is abruptly truncated by an underlying, virtually unweathered, pahoehoe layer whereas the younger flows show a more gradual decline in recognizable weathering features with increasing depth.

3. Methods

We dug backhoe pits that reached rock too solid to excavate; rock fragments chipped by the backhoe at the pit bottom were assumed to be the parent material for the weathering zone, which was sampled by horizon. The deepest pits reached slightly <5 m. Rainfall for each site was determined by interpolation between isohyets based on (Giambelluca et al., 1986) using ArcGIS 9.0. Samples were shipped to UC Santa Barbara, sieved through a 2-mm screen, ground, and analyzed for elemental composition by X-ray fluorescence (XRF) at ALSChemex (Sparks, NV). Duplicates yielded values within ~5% for all major elements and niobium. A subsample was ashed at 550 °C for 4 h to determine carbon and water content, reported as loss on ignition (LOI). We assumed that mass loss from coarse (>2 mm) fragments was zero, a simplifying approach that only affects our results for the youngest flow (where we can visually verify that the rock fragments are virtually unweathered) and the driest sites on the oldest flows (where we know that they are partly weathered, but are not abundant enough, or weathered enough, to affect our calculations) (Section 3.1, Table 1 in the Appendix).

3.1. Mass loss calculations

To determine mass loss or gain for a particular element, we compared the concentration of that element to niobium (Nb), which is one of the least mobile elements in Hawaiian soils (Kurtz et al., 2000). Other elements often used in immobile element studies, such as zirconium (Zr), are mobile enough as to be unreliable tracers in basalt-derived soils at the high rainfall end of our climosequences (S. Porder, unpubl. data). The fraction of element lost or gained from a particular soil horizon can be expressed as the function $\tau_{j,w}$ such that:

$$\tau_{j,w} = \left[\frac{C^*_{j,w}C_{Nb,p}}{C^*_{Nb,w}C_{j,p}} - 1\right] * ff \quad (1)$$

where $C_{j,w}$ is the concentration of element j in the weathered horizon, $C_{Nb,w}$ is the concentration of Nb in the weathered horizon, and the subscript p refers to parent material concentrations, and ff refers to the fraction of the soil mass in the <2 mm size range (Brimhall et al., 1992; Kurtz et al., 2000; Chadwick et al., 2003). This loss factor corrects for LOI, incorporates changes during soil dilation or collapse and the associated changes in bulk density, and allows us to determine, for each element individually or for the soil as a whole, what fraction of the original parent material mass remains in a particular weathered soil.

To determine total mass loss (δ_{total}), we summed the τ for each element weighted by the abundance of that element in parent material for a particular soil horizon of a given thickness. This value represents the fraction of mass lost from the parent material as it transformed into a particular horizon. We multiplied this fraction of mass loss in each horizon by the average bulk density of a'a tephra parent material in Hawai'i to arrive at the mass loss (rather than the fraction of mass loss) during the formation of a particular horizon. We then weighted the mass loss in each horizon by its thickness and summed over all horizons in the weathering zone. This allowed us to calculate δ_{total}, the mass lost per unit area for the entire weathering profile at a given site:

$$\delta_{\text{total}} = \sum_{i=1}^{n} \rho z_i \left(\sum_{j=1}^{m} (\tau_j C_{j,p})\right) \quad (2)$$

where n is the number of horizons in the pit, j is the number of elements, z_i is the thickness of horizon i, $C_{j,p}$ is the percentage of element j in the parent material, $\rho = 1.35$ (± 0.38) g cm^{-3}, the average bulk density of Hawai'i basalt (including void and infilled vesiculated tephra). We arrived at this bulk density estimate by averaging ten bulk density measurements of a'a clinkers, ten measurements of tephra bulk density, and estimating 40%±10% void space (which can then be filled by tephra) in a typical a'a flow. The uncertainty associated with this estimation is propagated through our mass loss calculations. Since our total mass loss calculations are based only on the <2 mm fraction, mass loss from coarser fragments will cause us to underestimate total mass loss, but only by a maximum of 9% (at the 170 ka,

570 mm yr^{-1} site) and much less at other sites (S. Porder, unpubl. data). This 9% calculation has some error, it is dependent on the parent material of the coarse fragments (a'a clinkers vs. tephra), and since the fraction fines are so high, and the mass loss from the coarse fragments quite low in most cases, the most robust calculation is of mass loss from the fines only. All mass losses are presented on an oxide basis.

We calculated the rate of mass loss from the 10 ka flow by dividing the total mass loss for a given rainfall site by 10 ka to arrive at an average mass loss rate over the first 10 ka of soil development. To calculate mass loss during the 10–170 ka interval at a given rainfall, we subtracted the mass lost from the 10 ka flow from the mass lost from the 170 ka flow, and then divided the remaining amount by 160 ka. A similar calculation was performed to determine loss rates during the 170–350 ka interval. These calculations assume a space for time substitution, and this assumption is discussed in Section 5.3.

3.2. Quantifying dust inputs

Terrestrial surfaces receive mineral aerosol that is often highly weatherable because of its high surface area (Simonson, 1995), and Hawai'i is no exception (Parrington et al., 1983). Accounting for mineral aerosols in weathering studies is difficult because often the inputs are of similar composition compared to the putative parent material (Brimhall et al., 1988; Simonson, 1995). Compared with the mantle-derived basaltic lavas of Hawai'i, however, we can quantify mineral aerosol inputs using mineralogy (quartz) and the isotopic tracers strontium (Sr) and neodymium (Nd) (Rex et al., 1969; Jackson et al., 1971; Chadwick et al., 1999; Kurtz et al., 2001; Stewart et al., 2001). In theory, we can estimate a net flux of mineral aerosol to known-age lava flows by quantifying the amount of non-lava minerals (i.e. quartz and mica; Jackson et al., 1971) accumulated in the soil profiles. However, there are several complications (discussed below) that make this calculation subject to considerable uncertainty. We quantified quartz and mica fluxes as follows: 1) Quartz and feldspar concentrations in soil were determined from the residue obtained from a sodium pyrosulfate fusion, a 3 M hydrochloric acid wash and boiling for 2.5 min in 0.5 M sodium hydroxide. The quartz content is based on the weight of the residue after correcting for the weight of the feldspars, which were determined from the calcium (Ca), sodium (Na) and potassium (K) in the residue. 2) Mica was determined from the total K in the residue after accounting for the K in feldspars (Chadwick et al., 1999; Jackson et al., 1986).

We converted quartz and mica concentrations to mass per volume using soil-horizon bulk density (measured using the clod–volume displacement method; Soil Survey Laboratory Staff, 1992) and converted mass of quartz + mica to mass dust by assuming that dust is composed of 30% quartz + mica. This assumption differs somewhat from ship-board measurements near Hawai'i that indicate that dust contains about 20% quartz and 30 to 50% mica on an X-ray amorphous-free basis (Leinen et al., 1994), values that obscure a large amount of variability controlled by both changes in source area and travel time (Arnold et al., 1998) as well as up to 30% material of unknown composition because its crystal structure is amorphous when viewed with X-ray diffraction. Other mineral components are plagioclase, kaolinite, smectite and chlorite (Leinen et al.,

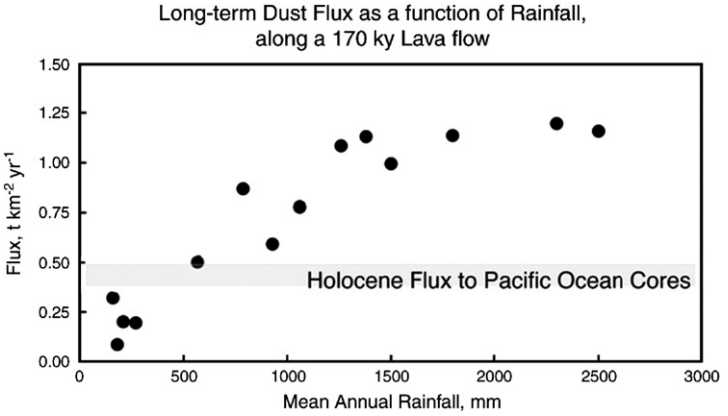

Fig. 2. Calculated flux of dust vs. rainfall on the 170 ka (Hawi) flow. Most of the dust is found in the upper 30 cm of the soil. A polynomial equation ($-2*10^{-7}x^2+0.001x-0.01$) yields an R^2 of 0.93, and was used to calculate the dust fluxes reported in the text. The Holocene dust flux reported here is from (Rea et al., 1994).

1994; Arnold et al., 1998), but these come in smaller quantities and are less recognizable against the lava background. For the Hawi lava flows under consideration here, Kurtz et al. (2001) verified a composition of 20% quartz and 10% mica using Nd isotopes as a complementary tracer to quartz for soils receiving 2500 mm of rainfall. We use 30% quartz plus mica of Kurtz et al. (2001), rather than the 50–70% value of Leinen et al. (1994), to account for the Nd isotopic work of Kurtz et al. (2001), and the non-quantified, X-ray amorphous fraction of the dust not accounted in the Leinen et al. (1994) study. The quartz plus mica fraction scales linearly with our total dust flux, so using the value of Leinen (~60%) would decrease our dust flux estimate by 50%.

We arrived at a long-term rate of dust deposition by dividing the mass of dust by the age of the flow (170 ka) (Fig. 2). This calculation assumes that quartz and mica have not weathered significantly since deposition. This is almost certainly valid for quartz and is reasonable for mica over the relevant timescales in this study (Kurtz et al., 2001). Weathering of dust minerals would lead us to underestimate the dust flux to a given site. Despite this possible underestimate, measured dust accumulation in the 170 ka soils is substantial, increasing from 330 to 2000 t ha^{-1} across the rainfall gradient. We fit the dust vs. rainfall curve from the 170 ka flow with a polynomial curve (Fig. 2, $R^2=0.93$), and used that curve to calculate that dust fluxes to all of our sites range between 0. 54 and 1.45 t km^{-2} yr^{-1}. The increase in dust with increasing rainfall fits well with previous descriptions of upper atmosphere transport and deposition of dust as condensation nuclei for raindrops (Parrington et al., 1983). Our highest dust flux values are similar to the flux calculated using Nd isotopes (1.25 t km^{-2} yr^{-1}) by Kurtz et al. (2001) for a nearby 170 ka site of comparable rainfall (the Kohala Long Substrate Age Gradient site described by Vitousek, 2004). Total dust flux appears to plateau at the wetter sites, either because of some weathering/erosion of dust or because high rainfall effectively scavenges most of the dust from the atmosphere at all of the high rainfall

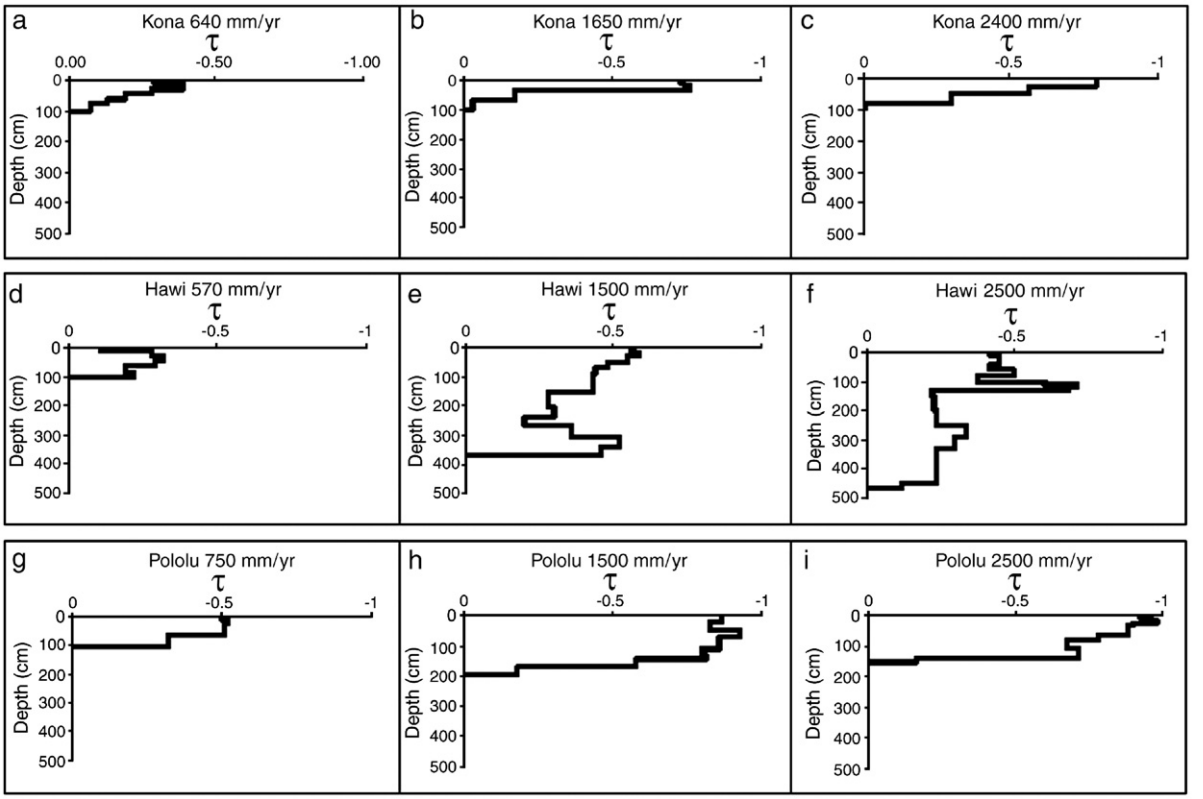

Fig. 3. Fraction of original mass lost from the <2 mm fraction (τ) from the 10 ka Kona (a–c), 170 ka Hawi (d–f), and 350 ka Pololu (g–i) flows at selected different rainfalls. Across each flow, mass loss increases with increasing rainfall, and total mass loss increases with flow age for a given rainfall. The full dataset of elemental composition and total mass loss values for each of the 28 sites is available in Table 1 of the Appendix. τ was calculated by calculating the mass loss fraction for each major element, and weighting the total τ by the composition of the parent material.

sites (Vitousek, 2004). Assuming that for a given rainfall the flux has been constant through time, we calculated the total dust inputs to the 10 ka Kona and 350 ka Pololu soils (this assumption is discussed in Section 5.3). This allows us to estimate dust accumulation on each of the flows, but we place the most emphasis on the dust results from the 170 ka flow for which we have the best data.

4. Results

The data from this age by climate matrix show a deepening and depleting weathering zone with increased age and precipitation (Fig. 3, Table 1 in the Appendix). The weathering zone is less than a meter deep at every site along the 10 ka surface, with high mass loss only in the upper ~25 cm (Fig. 3a–c). In

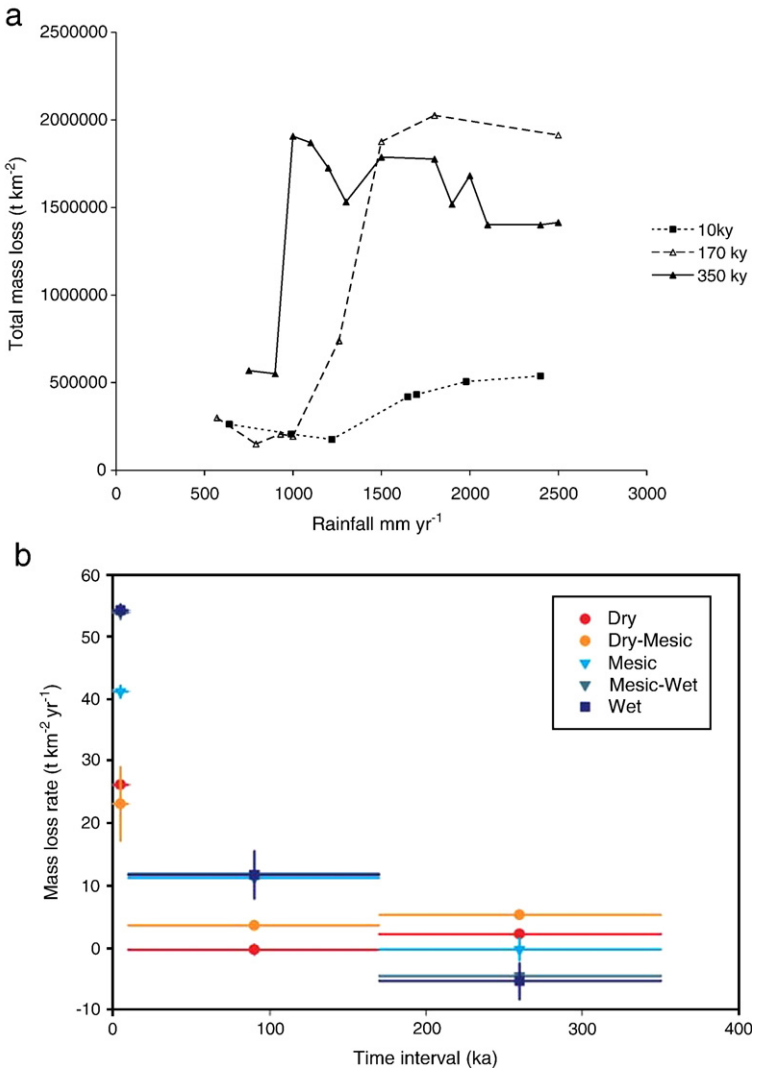

Fig. 4. a) Total mass lost from each flow under different climatic conditions. These values assume that the rock at the base of each backhoe-dug pit is the parent material. Note that the precipitation threshold above which mass loss increases substantially is dependent on flow age. The threshold occurs at ~1000 mm yr^{-1} on the oldest flow, but at ~1500 mm yr^{-1} on the youngest. b) The rate of mass loss for each time interval between the flows (0–10, 10–170–170–350 ka). Calculations and uncertainties are described in Sections 3.1 and 5.3. Dry sites include: an average of the 640 and 990 mm yr^{-1} site on the 10 ka flow, the 790 mm yr^{-1} site on the 170 ka flow, and the 750 mm yr^{-1} site on the 350 ka flow. Dry-mesic sites include the 1260 mm yr^{-1} site from the 10 ka flow, the 1220 mm yr^{-1} site from the 170 ka flow, and the 1200 mm yr^{-1} site on the 350 ka flow. Mesic sites include the 1500 mm yr^{-1} sites on each flow. Mesic-wet sites include the 1980 mm yr^{-1} site on the 10 ka flow, the 1800 mm yr^{-1} site on the 170 ka flow, and the 1900 mm yr^{-1} site on the 350 ka flow. Wet sites are the 2400 mm yr^{-1} site on the 10 ka flow, and the 2500 mm yr^{-1} sites on the older flows. *X* error bars span the interval for each calculated rate, and *Y* error bars include error associated with parent material choice (pit bottom or average of nearby outcrops; Table 1 and Section 5.3) and with bulk density determinations (Section 3.1).

contrast, the weathering zone on the 170 ka flow reaches almost 5 m in depth with substantial (>25%) mass loss even at 4 m depth under the wettest conditions (Fig. 3f). On the 350 ka flow, the weathering zone overlies an almost completely unweathered pahoehoe flow at ~2 m depth, but mass loss above this barrier approaches 100% at rainfalls above ~1000 mm yr^{-1} (Fig. 3g–i). As mentioned previously, weathering rates of pahoehoe are much slower than of a'a/tephra type flows, and this lithologic transition diminishes the total mass loss values from the oldest sites. Total mass loss from the weathering zone increases with precipitation as the weathering zone deepens and progressively depletes (Fig. 4). However, this relationship is non-linear, on each flow there is a precipitation threshold above which total mass loss increased substantially. The threshold precipitation decreases from ~1500 mm yr^{-1} on the 10 ka flow to ~1000 mm yr^{-1} on the 350 ka flow (Fig. 4a).

Mass loss rates drop dramatically after the first 10 ka of weathering: from ~54 t km^{-2} yr^{-1} at the wet site during the first 10 ka to 11.8 t km^{-2} yr^{-1} averaged over the next 160 ka (Fig. 4b). Rates on the dry sites are substantially lower, averaging 26 t km^{-2} yr^{-1} over the first 10 ka of soil development and dropping to near zero thereafter (Fig. 4b). We calculated negative mass loss rates for the wet sites during the 170–350 ka interval. These are a result of the truncated weathering zone on the oldest flow. Total mass loss from the 170 ka flow, where the weathering zone is not truncated, is greater than from the truncated weathering zone on the 350 ka flow. Subtracting the former from the latter, and then dividing by the time interval between the flows, yields a negative mass loss rate. The rate of mass loss at the dry

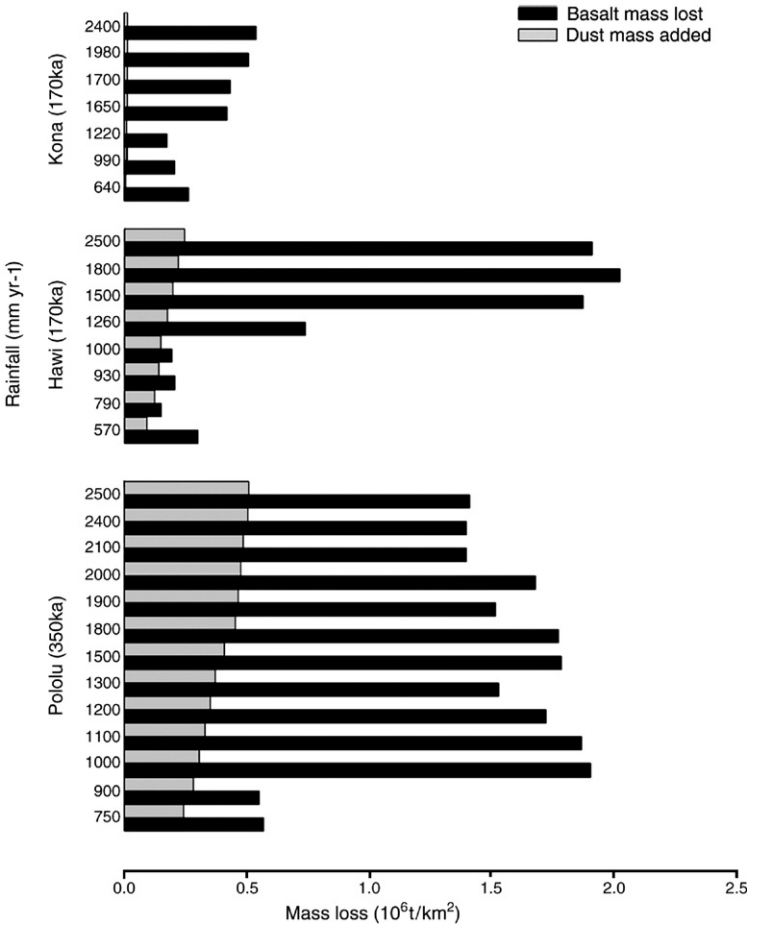

Fig. 5. The mass loss via basalt weathering (black bars) and mass gain via dust addition (grey bars) for the entire weathering zone for each flow. Rainfall increases up the *y*-axis for each flow. Dust values were calculated by determining the rate of flux to the 170 ka flow, and extrapolating this rate to the 10 and 350 ka flow (as described in Section 3.2).

(<1000 mm yr^{-1}) sites, where weathering depth is less impacted by the lithologic transition below the 350 ka flow, is similar during the 10–170 and 170–350 ka intervals (Fig. 4b).

Surprisingly, inputs of exogenous dust to the older flows are of a similar order of magnitude as chemical weathering losses from the parent material. On the 170 ka flow, where there is the best constraint on dust mass added, dust inputs average 30%±24% (1SD) of the mass lost to chemical weathering. At rainfalls less than 1000 mm yr^{-1} dust inputs reach ~80% of mass loss from parent material (Fig. 5).

5. Discussion

5.1. Mass loss

The rapid decline in mass loss rates seen in these data can be attributed to the minimal rates of physical erosion. With no nearby streams to export material, low slopes, and our sampling of slightly concave portions of otherwise slightly convex landscapes, particulate loss caused by overland flow is likely to be minimal. While wind erosion is possible, in the wet sites it is likely to be low because of plant cover, and in the drier sites the soils are protected from wind erosion by a rock pavement (Chadwick et al., 1999). Without the physical removal of weathered substrate, the chemical weathering rates on these minimally eroded flows decrease — for a given rainfall the 10–170 ka interval averages mass loss rates ~5 to 10 times lower than those during the first 10 ka (Fig. 4b). This result is consistent with those from a chronosequence of Hawaiian sites receiving 2500 mm yr^{-1} rainfall, where weathering rates drop off steeply between 2.1 and 20 ka (Vitousek, 2004). Even during the earliest interval (0–10 ka), mass loss rates are well within the range measured for actively eroding granitic catchments (Riebe et al., 2004), despite the greater reactivity of basaltic parent material. Reported weathering rates from basaltic catchments vary widely, but are in the upper range and above the values reported here (Dessert et al., 2001). This supports the idea that physical weathering is a prime driver of chemical denudation, and further argues that catchments that show higher chemical weathering fluxes than we see here may have mean soil residence times of <10 ka.

We are not able to ascertain how much loss rates decrease at wet sites during the 170–350 ka interval. As a result of the truncation of the weathering zone at a lithologic transition, our total mass losses from the oldest flow are minimum values. This is highlighted by the higher weathering rates at dry, rather than wet, sites during the 170–350 ka interval (Fig. 4b), an artifact of the truncation of the weathering zone at the wetter sites. To investigate the effect of this truncation on measured 350 ka flow mass losses, we sampled the weathering zone on a similar-aged a'a flow that receives ~1800 mm yr^{-1} but where the weathering zone is ~3.5 m and overlies a buried soil. Mass loss from this profile is ~43% greater than in the equivalent profile at 1800 mm yr^{-1} rainfall along our 350 ka transect, indicating that our mass loss values are affected by the truncated weathering zone by at least this much (Fig. 6). Using this larger mass loss value in our rate calculations indicates that the mass loss rate during the 170–350 ka interval is about one-third of the rate during the 10–170 ka interval at 1800 mm yr^{-1} rainfall.

Total mass loss increases substantially above the threshold where total precipitation (Pt) exceeds evapotranspiration (ET), as previously described by (Chadwick et al., 2003). Interestingly, the rainfall at which the threshold occurs lowers as the flows age (Fig. 4a). We can think of two plausible explanations: 1) past climate

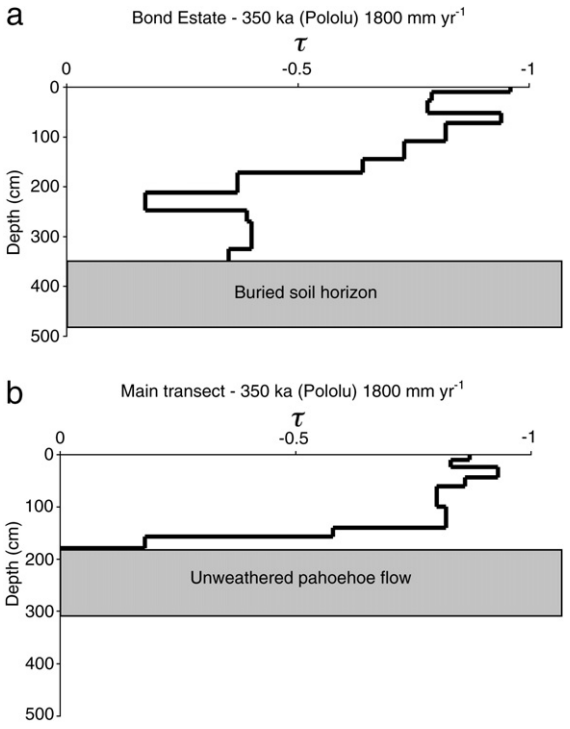

Fig. 6. a) Mass loss from a 350 ka Pololu flow with a mean annual rainfall of 1800 mm yr^{-1} but where there is no lithologic or hydrologic barrier at shallow depth, as there is in our main transect. This still does not represent total potential mass loss after 350 ka, because the flow overlies a buried soil at 3.5 m depth. b) Mass loss from the comparable 1800 mm yr^{-1} site on our main 350 ka transect, where the a'a/tephra flow overlies a virtually unweathered pahoehoe flow at 1.8 m depth.

shifts have not been consistent between the flows or 2) older flows have experienced more anomalously wet years. Where Pt ~ ET (~1500 mm yr^{-1} at these sites), water flow through the weathering zone and concomitant chemical depletion of soil may occur mainly during unusually wet years. Older sites, having experienced a greater number of unusually wet years, may therefore be more weathered than younger sites situated at similar modern day rainfall. Even the dry sites show progressive element losses, albeit at considerably slower rates. Chadwick et al. (in press) suggest that to the extent mass is lost at all via physical processes, the dominant vector at drier sites is not driven by water flux (which is minimal), but rather removal of material via wind. If this is the case, wind is likely to remove dust as well, since dust is deposited on the soil surface (discussed below).

5.2. Dust

These data also highlight the potential importance of dust as a chemically weatherable substrate. In Hawai'i, silicate rich dust does not weather as fast as mafic volcanic ash and tephra, and thus dust accumulates even as parent material becomes depleted. However on continents, dust and bedrock composition are often more similar, and there is every reason to suspect that fine-grained particulates deposited at the surface present a highly weatherable substrate relative to local bedrock. Our calculated dust mass inputs for the 170 ka flow are within an order of magnitude of the total mass lost through chemical weathering of that flow. This calculation is quite conservative, since we assume no dissolution of quartz and mica since deposition, and since there is likely to be some dust lost to wind erosion (Vitousek, 2004). Dust deposition in the open ocean around Hawai'i is two to three orders of magnitude lower than closer to the continents (Rea, 1994). Although the islands scavenge dust through the creation of orographic rainfall, many continental settings are still two to three orders of magnitude dustier than Hawai'i (Kurtz et al., 2001; Okin et al., 2003 and references therein). If the dust mass added to this relatively non-dusty, 170 ka flow is close to chemical weathering losses, it begs the question of whether dust inputs are an important driver of chemical weathering fluxes on continents.

Okin et al. (2003) modeled global dust fluxes on continents that ranged from ~0.1 to 100 t km^{-2} yr^{-1}. This range is similar to the range of weathering fluxes from many catchments worldwide (Bluth and Kump, 1994; White and Blum, 1995; Gíslason et al., 1996; Jacobson et al., 2003; Riebe et al., 2004; Das et al., 2005), though larger fluxes occur on the island of Réunion (Louvat and Allégre, 1997). Thus it seems plausible that in some catchments a substantial fraction of measured chemical denudation is supplied by dust weathering, with the rest coming from the physical degradation, and subsequent chemical weathering, of bedrock. The magnitude of this fraction will depend heavily on both substrate and dust mineralogy, as well as climate, vegetation, and erosion rates. Mineralogy may be particularly important. Quartz-dominated dust that lands on mafic volcanics may not contribute substantially to the overall weathering flux, but dust rich in weatherable minerals that lands on relatively recalcitrant bedrock has the potential to be of considerable importance.

5.3. Uncertainties

This investigation utilized variability in three factors across our sites: flow age, rainfall, and dust deposition. The uncertainty in age determination has been discussed in detail by Chadwick et al. (2003), so we will focus here on the latter two. We arrived at modern day rainfall values by interpolating between isohyets, but Kohala mountain experiences a 15 fold drop in rainfall over ~10 km, and there are too few rain gauge stations to determine the isohyets with a high degree of certainty. We have absolute certainty as to the relative rainfall between sites across a flow, this is determined by proximity to the top of Kohala mountain and the strong orographic control of precipitation. But the absolute values are not as well constrained, and we estimate that the rainfall values reported for a given site are accurate within 200–300 mm yr^{-1}.

While we have a good understanding of modern rainfall across our gradients, paleoclimatic variability is harder to constrain. Hotchkiss et al. (2000) have argued that rainfall at upper elevation sites on Kohala mountain (the site of the 170 and 350 ka flows) was as much as 50% lower than present day during much of the past 150 ka. The lower elevation sites on Kohala have likely been quite dry (as they are today) over the past few hundred thousand years and thus the rainfall gradient across a given flow has likely been less extreme for much of the flow history than it is today (Chadwick et al., 2003). Nevertheless, the intertwining of the 170 ka and 350 ka flows strongly favors the hypothesis that they have experienced similar climatic fluctuations through their shared history. Pollen evidence from Kohala suggests that climate has been more stable during the Holocene than previously (Chadwick et al., 2003). Although our 10 ka flow is not on Kohala Mountain, it is nearby (Fig. 1), and the present day

climate across the 10 ka flow is likely representative of its entire history.

In addition to variation in rainfall, the older flows may have experienced higher fluxes of Asian dust during glacial times (Chadwick et al., 1999; Kurtz et al., 2001; Chadwick et al., 2003). We determined the long-term dust flux across the rainfall gradient on the 170 ka flow, a flux that averages glacial–interglacial variation. Our approximation that the rainfall dependence of dust deposition rates is similar between flows, and that rates have been constant through time, may hold well for the 170 ka and 350 ka flow. However dust fallout over the open ocean varies by a factor of 3 to 5 over glacial–interglacial cycles (Rea, 1994; Rea et al., 1994), which argues that the dust flux to the 10 ka flow is likely substantially lower than the fluxes experienced by the older flow. Nonetheless, our assumption of constant flux through time allows us to estimate, within a factor of 3 to 5, how dust deposition compares with mass loss via chemical weathering on the younger flow. We also make the assumption that quartz and mica have not significantly weathered during development of the 170 ka weathering zones, an assumption that makes our dust mass calculations conservative and the substantial accumulation of dust relative to parent material depletion all the more surprising.

Finally, the assumption that all of our weathering profiles started as similar parent material is reasonable (they were originally a'a Hawaiian basalts), but geochemical variation between the basalts is an important source of uncertainty. In particular, all of our mass loss calculations depend on an accurate assessment of parent material composition and Nb concentration. We chose to define "unweathered" parent material as the layer at the bottom of each pit that the backhoe could not break through. In every pit this appeared to be unaltered bedrock; the average SiO_2 content of the pit bottoms of each flow was >45%. Alternatively, we could have chosen nearby "unweathered" basalts and arrived at an average parent material value for each flow (as in Chadwick et al., 2003). There is no guarantee that the hard rock at the base of each weathering zone is the same chemical composition as the overlying mixed lava and tephra from which most of the weathering zone formed. On the other hand, finding solid, unaltered basalt in road cuts near our sites presents a similar difficulty because large clasts of unweathered basalt are almost certainly not the material that formed the majority of the weathering zone. By repeating our calculations using average parent material values from each flow, we calculated that the mean shift in mass loss associated with parent material choice is 7%±19% (1SD) (Table 1). This variation is included in the mass loss rate error bars (Fig. 4b).

For the 10 ka flow, the choice of parent material is further complicated by its proximity to Hualalai Volcano, which has covered 80% of its shield surface with new flows in the past 5000 years (Wolfe and Morris, 1996). Ash from the alkalic Hualalai eruptions has higher Nb concentrations than the thoelitic Kona flow, thus significant inputs of ash from Hualalai could increase the calculated total mass loss, and mass loss rates, based on the Kona flow values. While we acknowledge this potential underestimate, we have not quantitatively assessed Hualalai ash inputs to the Kona flow, and our calculations assume no input of ash from Hualalai. Despite the uncertainties on the youngest flow, there is good evidence that post-extrusion tephra inputs are not a significant source of error for the older-flow

Table 1
Total mass loss from each of the 28 sites

Flow age (ka)	Rainfall (mm yr^{-1})	Total mass loss (t km^{-2})	Total mass loss (t km^{-2})
10	640	**262,500**	*318,800*
10	990	**206,350**	*181,250*
10	1220	**175,000**	*266,250*
10	1650	**418,750**	*406,250*
10	1700	**431,250**	*443,750*
10	1980	**506,250**	*493,750*
10	2400	**537,500**	*550,000*
170	570	**300,000**	*356,300*
170	790	**150,000**	*281,300*
170	930	**206,300**	*218,800*
170	1000	**193,800**	*231,300*
170	1260	**738,400**	*863,600*
170	1500	**1,875,000**	*2,433,100*
170	1800	**2,025,000**	*2,668,800*
170	2500	**1,912,500**	*2,812,500*
350	750	**568,800**	*693,800*
350	900	**550,000**	*656,000*
350	1000	**1,906,000**	*2,013,000*
350	1100	**1,869,000**	*2,031,000*
350	1200	**1,725,000**	*1,762,500*
350	1300	**1,531,000**	*1,590,000*
350	1500	**1,787,500**	*1,887,500*
350	1800	**1,775,000**	*1,800,000*
350	1900	**1,518,800**	*1,593,800*
350	2000	**1,681,000**	*1,881,000*
350	2100	**1,400,000**	*1,510,000*
350	2400	**1,400,000**	*1,487,500*
350	2500	**1,413,000**	*1,469,000*

Bolded column indicates mass loss as calculated using pit-bottom material as parent material. These values were used as the basis of discussion throughout the text. Plain text column indicates mass loss values as calculated using average outcrop values from each flow as parent material for the sites on that flow. Italic column indicates mass loss values using nearby blue-rock basalt as parent material.

calculations. The vast majority of the Asian dust in the profile is found in the upper 30 cm, which would not be the case if these flows were continually recovered with blankets of tephra. In addition, the two older flows are up wind from all subsequent extant volcanoes on Hawaii and we see no evidence for substantial input of tephra from these subsequent eruptions. However, we can detect the addition of 170 ka Hawi tephra to the 350 ka Pololu flows in the soil stratigraphy. We chose to not correct for the layering effect, because we did not trust we could do that without introducing more uncertainty than we resolved.

Dust affects the mass loss calculations indirectly, because it adds both mass and Nb to the profile. Fortunately, the Si:Nb of dust is similar to that of the 170 and 350 ka flows, where dust accumulation is significant, and thus to a first approximation our mass loss values do not need to be adjusted to account for the extra Nb. This undoubtedly creates uncertainty in our quantification of dust and mass loss fluxes, but not enough to call into question the conclusion that dust inputs are of a similar order of magnitude to chemical weathering losses in our older sites.

There are two important points that need to be raised in light of these uncertainties. The two dominant signals in this study, a steep drop in chemical weathering rates with time and the rising relative magnitude of dust fluxes to chemical weathering losses on older surfaces, are observable despite the inherent uncertainties. More broadly, our study area is far from unique in the complications it presents for quantifying long-term chemical weathering rates. Rather, the unique aspects of the Hawaiian system allow us to assess the relative importance of dust inputs, mass losses, and parent material heterogeneity in a more quantitative framework than perhaps is possible in any other system.

6. Conclusion

The role of chemical weathering in driving atmospheric CO_2 concentrations, and thus Earth's climate, makes understanding the proximate control of weathering rates of singular importance. While physical removal of weathered material clearly promotes chemical weathering, disentangling the role of climate has been a complicated endeavor (Von Blanckenburg, 2005). By working in minimally eroded settings, we have demonstrated that chemical weathering rates decline steeply over time in the absence of physical erosion to levels much lower than observed in basaltic catchments worldwide (Dessert et al., 2003). The measurement of high weathering rates (higher even than during our 0–10 ka interval) in granitic catchments argues strongly that the mean soil residence times in these catchments are quite short, in agreement with data from cosmogenic nuclide studies (Riebe et al., 2004). In addition, by minimizing the overprint of physical denudation, we were able to observe that the relationship between chemical weathering and climate is non-linear. As soon as precipitation exceeds potential evapotranspiration, weathering rates increase dramatically compared with drier sites. Increased rainfall beyond this threshold has little effect on weathering rates.

Our results highlight another potential driver of chemical weathering rates that has received limited discussion: dust deposition. Unlike most catchment-scale studies, which at best can quantify short-term dust deposition, we have measured long-term average rates and, surprisingly, found them comparable to chemical denudation of the parent material. In Hawai'i, dust is relatively recalcitrant compared with parent material, hence it accumulates in the surface soil horizons even as the parent material is broken down and lost through leaching or other mechanisms. By contrast, many continental catchments receive orders of magnitude more dust that is often of similar chemical composition, and smaller grain size, than the underlying parent material. These fine-grained minerals lie near the surface where soil solution is most acidic and therefore becomes the locus of weathering, providing considerable protection to the rock minerals below. Most studies of weathering at the catchment scale have missed the importance of dust as a significant contributor to weathering flux. It is possible that patterns of dust deposition, past and present, play an important role in determining chemical weathering rates globally and in individual studies may explain otherwise anomalous results.

Appendix A. Supplementary data

Supplementary data associated with this article can be found, in the online version, at doi:10.1016/j.epsl.2007.03.047.

References

Anderson, S.P., Dietrich, W.E., Brimhall Jr., G.H., 2002. Weathering profiles, mass-balance analysis, and rates of solute loss: linkages between weathering and erosion in a small, steep catchment. Geol. Soc. Amer. Bull. 114, 1143–1158.

Arnold, E., Merril, J., Leinen, M., King, J., 1998. The effect of source area and atmospheric transport on mineral aerosol collected over the North Pacific Ocean. Glob. Planet. Change 18, 137–159.

Basu, A.R., Jacobsen, S.B., Poreda, R.J., Dowling, C.B., Aggarwal, P.K., 2001. Large groundwater strontium flux to the oceans from

the Bengal Basin and the marine strontium isotope record. Science 293, 1470–1473.
Berner, R.A., Lasaga, A.C., Garrels, R.M., 1983. The carbonate–silicate geochemical cycle and its effect on atmospheric carbon dioxide over the past 100 million years. Am. J. Sci. 283, 641–683.
Bluth, G.J.S., Kump, L.R., 1994. Lithologic and climatologic controls of river chemistry. Geochim. Cosmochim. Acta 58, 2341–2359.
Brimhall, G.H., Lewis, C.J., Ague, J.J, Dietrich, W.E., Hampel, J., Teague, T., Rix, P., 1988. Metal enrichment in bauxites by deposition of chemically mature aeolian dust. Nature 333, 819–824.
Brimhall, G.H., Chadwick, O.A., Lewis, C.J., Compston, W., Williams, I.S., Danti, K.J., Dietrich, W.E., Power, M.E., Hendricks, D., Bratt, J., 1992. Deformational mass transport and invasive processes in soil evolution. Science 255, 695–702.
Carey, A.E., Lyons, W.B., Owen, J.S., 2005. Significance of landscape age, uplift, and weathering rates to ecosystem development. Aquat. Geochem. 11, 215–239.
Chadwick O.A., Kelly E.F., Hotchkiss S.C., Vitousek P.M., Precontact vegetation and soil nutrient status in the shadow of Kohala Volcano, Hawai'i. Geomorphology (in press). doi:10.1016/j.geomorph.2006.07.023.
Chadwick, O.A., Derry, L.A., Vitousek, P.M., Huebert, B.J., Hedin, L.O., 1999. Changing sources of nutrients during four million years of ecosystem development. Nature 397, 491–497.
Chadwick, O.A., Gavenda, R.T., Kelly, E.F., Ziegler, K., Olson, C.G., Elliott, W.C., Hendricks, D.M., 2003. The impact of climate on the biogeochemical functioning of volcanic soils. Chem. Geol. 202, 195–223.
Das, A., Krishnaswami, S., Sarin, M.M., Pande, K., 2005. Chemical weathering in the Krishna Basin and Western Ghats of the Deccan Traps, India: rates of basalt weathering and their controls. Geochim. Cosmochim. Acta 69, 2067–2084.
Dessert, C., Dupré, B., Gaillardet, J., François, L.M., Allègre, C.J., 2003. Basalt weathering laws and the impact of basalt weathering on the global carbon cycle. Chem. Geol. 202, 257–273.
Dessert, C., Dupré, B., François, L.M., Schott, J., Gaillardet, J., Chakrapani, G., Bajpai, S., 2001. Erosion of Deccan Traps determined by river geochemistry: impact on the global climate and the $^{87}Sr/^{86}Sr$ ratio of seawater. Earth Planet. Sci. Lett. 188, 459–474.
Giambelluca, T.M., Schroeder, T.A., 1998. Climate. In: Juvik, S.P., Juvik, J.O., Paradise, R.R. (Eds.), Atlas of Hawai'i, (3rd ed.). pp 49–59.
Giambelluca, T.M., Nullet, M.A., Schroeder, T.A., 1986. Rainfall Atlas of Hawai'i. State of Hawai'i Department of Land and Natural Resources, Honolulu. Report R76.
Gíslason, S.R., Arnórsson, S., Ármannsson, H., 1996. Chemical weathering of basalt in southwest Iceland: effects of runoff, age of rocks and vegetative/glacial cover. Am. J. Sci. 296, 837–907.
Hedin, L.O., Vitousek, P.M., Matson, P.A., 2003. Nutrient losses over four million years of tropical forest development. Ecology 84, 2231–2255.
Hotchkiss S, Quaternary vegetation and climate of Hawai'i. Ph.D. Dissertation, University of Minnesota, St. Paul. (1998).
Hotchkiss, S.C., Vitousek, P.M., Chadwick, O.A., Price, J.P., 2000. Climate cycles, geomorphological change, and the interpretation of soil and ecosystem development. Ecosystems 3, 522–533.
Jackson, M.L., Lim, C.H., Zelzny, L.W., 1986. Oxides, hydroxides and aluminosilicates. Methods of Soil Analysis: Part I. Physical and Mineralogical Properties. 2nd ed. of Agronomy, vol. 9, pp. 102–149.
Jackson, M.L, Levelt, T.V.M., Syers, J.K., Rex, R.W., Clayton, R.N., Sherman, G.D., Uehara, G., 1971. Geomorphological relationships of tropospherically derived quartz in the soils of the Hawaiian Islands. Soil Sci. Soc. Am. Proc. 35, 515–525.
Jacobson, A.D., Blum, J.D., 2003. Relationship between mechanical erosion and atmospheric CO2 consumption in the New Zealand Southern Alps. Geology 31, 865–868.
Jacobson, A.D., Blum, J.D., Chamberlain, C.P., Craw, D., Koons, P.O., 2003. Climatic and tectonic controls on chemical weathering in the New Zealand Southern Alps. Geochim. Cosmochim. Acta 67, 29–46.
Jenny, H., 1941. Factors of Soil Formation: a System for Quantitative Pedology. McGraw Hill, New York.
Kurtz, A.C., Derry, L.A., Chadwick, O.A., 2001. Accretion of Asian dust to Hawaiian soils: isotopic, elemental and mineral mass balances. Geochim. Cosmochim. Acta 65, 1971–1983.
Kurtz, A.C., Derry, L.A., Chadwick, O.A., Alfano, M.J., 2000. Refractory element mobility in volcanic soils. Geology 28, 683–686.
Leinen, M., Prospero, J.M., Arnold, E., Blank, M., 1994. Mineralogy of the Aeolian dust reaching the North Pacific Ocean: 1) sampling and analysis. J. Geophys. Res. 99 (D10) 21017–21023.
Likens, G.E., 2004. Some perspectives on long-term biogeochemical research from the Hubbard Brook ecosystem study. Ecology 85, 2355–2362.
Louvat, P., Allégre, C.J., 1997. Present denudation rates on the island of Réunion determined by river geochemistry: basalt weathering and mass budget between chemical and mechanical erosion. Geochim. Cosmochim. Acta 61, 3645–3669.
McDougall, I., 1964. Potassium–argon ages of lavas from the Hawi and Pololu Volcanic Series, Kohala Volcano, Hawai'i. Geol. Soc. Amer. Bull. 75, 2597–2600.
McDougall, I., Swanson, D.A., 1972. Potassium–argon ages of lavas from the Hawi and Pololu Volcanic Series, Kohala Volcano, Hawai'i. Geol. Soc. Amer. Bull. 83, 3731–3738.
McEldowney H., A description of major vegetation patterns in the Waimea–Kawaihae region during the early historic period. Pp 407–448. In: Archaeological Investigations of the Mudlane–Waime–Kawaihae Road Corridor, Island of Hawai'i. Honolulu, Hawai'i, Dept. of Anthropology, Bernice Pauahi Bishop Museum (1983).
Okin, G.S., Mahowald, N., Chadwick, O.A., Artaxo, P., 2003. Impact of desert dust on the biogeochemistry of phosphorus in terrestrial ecosystems. Glob. Biogeochem. Cycles 18, GB2005. doi:10.1029/2003GB002145.
Parrington, J.R., Zoller, W.H., Aras, N.K., 1983. Asian dust: seasonal transport to the Hawaiian Islands. Science 220, 195–197.
Raymo, M.E., Ruddiman, W.F., 1992. Tectonic forcing of late Cenozoic climate. Nature 359, 117–122.
Rea, D.K., 1994. The paleoclimatic record provided by Eolian deposition in the deep sea: the geologic history of wind. Rev. Geophys. 32, 159–195.
Rea, D.K., Hovan, S.A., Janecek, T.R., 1994. Late Quaternary flux of eolian dust to the pelagic ocean. In: Hay, W.W. (Ed.), Geomaterial Fluxes, Glacial to Recent. National Academy Press, Washington D.C.
Rex, R.W., Syers, R.K., Jackson, M.L., Clayton, R.N., 1969. Eolian origin of quartz in soils of the Hawaiian Islands and in Pacific pelagic sediments. Science 163, 277–279.
Riebe, C.S., Kirchner, J.W., Finkel, R.C., 2004. Erosional and climatic effects on the long-term chemical weathering rates in granitic landscapes spanning diverse climate regimes. Earth Planet. Sci. Lett. 224, 547–562.
Simonson, R.W., 1995. Airborne dust and its significance to soils. Geoderma 65, 1–43.

Soil Survey Laboratory Staff, 1992. Soil Survey Laboratory Methods Manual. Soil Survey Investigations Report no. 42, v.2.0, USDA, Lincoln, NE.

Spengler, S.R., Garcia, M.O., 1988. Geochemistry of the Hawi lavas, Kohala Volcano, Hawai'i. Contrib. Mineral. Petrol. 99, 90–104.

Stallard, R.F., 1995. Tectonic, environmental, and human aspects of weathering and erosion: a global review using a steady-state perspective. Annu. Rev. Earth Planet. Sci. 23, 11–39.

Stewart, B.W., Capo, R.C., Chadwick, O.A., 2001. Effects of rainfall on weathering rate, base cation provenance, and Sr isotopic composition of Hawaiian soils. Geochim. Cosmochim. Acta 65, 1087–1099.

Taylor, A., Blum, J.D., 1995. Relation between soil age and silicate weathering rates determined from the chemical evolution of a glacial chronosequence. Geology 23, 979–982.

Vitousek, P.M., 2004. Nutrient Cycling and Limitation: Hawai'i as a Model System. Princeton University Press, Princeton, N.J. 223 pp.

Von Blanckenburg, F., 2005. The control mechanisms of erosion and weathering at basin scale from cosmogenic nuclides in river sediments. Earth Planet. Sci. Lett. 237, 462–479.

Wardle, D.A., Walker, L.R., Bardgett, R.D., 2004. Ecosystem properties and forest decline in contrasting long-term chronosequences. Science 305, 509–513.

White, A.F., Blum, A.E., 1995. Effects of climate on chemical weathering in watersheds. Geochim. Cosmochim. Acta 59, 1729–1747.

White, A.F., Brantley, S.L., 1995. Chemical weathering rates of silicate minerals: an overview. Rev. Mineral. 31, 1–22.

White, A.F., Brantley, S.L., 2003. The effect of time on the weathering of silicate minerals. Why do weathering rates differ in the laboratory and the field? Chem. Geol. 202, 479–506.

Wilkinson, B.H., 2005. Humans as geologic agents: a deep time perspective. Geology 33, 161–164.

Wolfe, E.W., Morris, J., 1996. Geologic map of the Island of Hawai'i. US Geological Survey Map 1-2524-A.